Report No.
UCB/SEMM-99/02

STRUCTURAL ENGINEERING,
MECHANICS AND MATERIALS

A Mixed-Enhanced Formulation for Tetrahedral Finite Elements

by

Robert L. Taylor

January 1999

DEPARTMENT OF CIVIL ENGINEERING
UNIVERSITY OF CALIFORNIA, BERKELEY
BERKELEY, CALIFORNIA

A Mixed-Enhanced Formulation for Tetrahedral Finite Elements

Robert L. Taylor *

Report No. UCB/SEMM-99/02

Abstract

This paper considers the solution of problems in three dimensional solid mechanics using tetrahedral finite elements. A formulation based on a mixed-enhanced treatment involving displacement, pressure and volume effects is presented. The displacement and pressure are used as nodal quantities while volume effects and enhanced modes belong to individual elements. Both small and finite deformation problems are addressed and sample solutions are given to illustrate the performance of the formulation.

1 Introduction

The use of low order triangular elements to solve problems in elasticity dates to the earliest years of the finite element method. In 1943 Courant employed triangular elements to present a variational solution to a St. Vennant torsion problem [8]. Engineering solutions of plane stress problems by composite triangular elements assembled to form a quadrilateral are presented by Turner *et. al.* in 1956 [24]. Solution to three dimensional problems using tetrahedral elements appeared in the early works of Argyris [1, 2], Gallagher [9], Melosh [15], and Rashid [16]. Although these elements have been available since these early dates it is well known that they cannot be used to solve problems in which an incompressible or nearly incompressible behavior is present. This failure may be assessed numerically by patch tests [29] or mathematically by the Babuška-Brezzi conditions [6, 13].

An equivalent of the incompressible linear elastic problem is given in fluid mechanics by the Stokes problem. The Stokes problem commonly is expressed in terms of a pressure and a velocity field, whereas, the equivalent incompressible linear elasticity problem is expressed by a pressure and a displacement field. Solution of the Stokes problem by finite element methods has an extensive literature. Several forms have been proposed to solve the problem using low order triangular and tetrahedral elements.

*Department of Civil and Environmental Engineering, University of California at Berkeley, Berkeley, California 94720-1710, e-mail: rlt@ce.berkeley.edu

Approaches based on a split of the governing equations have been proposed. This split concept was introduced by Chorin [7] and the observation that it permitted equal order interpolations was first observed by Schneider *et. al.* [19]. Several others have employed a split of the equations to solve problems in fluid mechanics (e.g., [18] and [26, 27]). A split of the equations has also been used to solve problems in solid mechanics in which an explicit time integration scheme is used [28]. A similar technique employing a nodal averaging of pressures on the split has been proposed by Bonet and Burton [5].

In approaches which do not rely on a split of the equations, an early element, often referred to as the MINI element, is given by Arnold *et. al.* in [3]. To satisfy the Babuška-Brezzi condition a mixed form involving the pressure and the velocity also is used. The pressure is approximated by a C^0 continuous linear interpolation and the velocity field also is a C^0 linear interpolation augmented by a cubic bubble function. The cubic bubble function appears in the inertial terms resulting in need to include specific knowledge of the transient integration scheme within each element. The element is also employed to solve the incompressible Navier-Stokes problem where the bubble term is essential to satisfy both the BB condition and to control the diffusive behavior of the convective terms.

Hughes *et. al.* [12] solve the Stokes problem with equal order interpolations for the pressure and velocity by employing a Petrov-Galerkin method augmented by Galerkin least square (GLS) stabilizing terms. Later an improved form is given which is symmetric for all admissible approximations [11]. In addition to equal order interpolations it is now permitted to use discontinuous pressure approximations. In the discontinuous form jump conditions in terms of pressures appear along boundaries of elements. In this form the computation of the finite element arrays involve multiple elements to form the pressured part. The equal order interpolation form of the formulation has very similar structure to the MINI element with differences only in the stabilizing terms. In the MINI element the bubble provides the stabilization, whereas in the Petrov-Galerkin form the GLS terms provide the necessary stabilization. Both forms involve transient terms in the stabilization parts and thus usually require treatment of time integration terms at the element level.

As noted above many of the successful finite element solutions for the Stokes problem have employed elements which employ continuous pressures and velocity fields. The natural formulation for the problem is a two-field variational form of the Reissner type (e.g., [17]). In non-linear solid mechanics, the use of a two-field variational form is not convenient for many constitutive models (e.g., hyperelastic models can have multiple deformation states for the same stress level - leading to non-unique states for a given stress). The use of a three-field variational form of the Hu-Washizu type (e.g., [25]) are in these cases more convenient. This form employs approximations of displacement, stress, and strain. The disadvantage in using a Hu-Washizu form appears at the fully incompressible limit where terms with infinite value appear. Here the Reissner form involves terms which have zero limit values and, thus, is more attractive for the limit case. The difficulty may be overcome in the three-field form by employing an Uzawa algorithm on a nearly incompressible problem (e.g., [4, 29]). The use of three-field approximations has led to successful low-order elements which may be used to solve the nearly incompressible problem for a wide range of constitutive models [20, 21, 22, 23].

In the present work we consider the solution of problems in solid mechanics using low

order tetrahedral elements. Both small and finite deformation formulations are considered. A three-field form involving continuous displacements and pressures and discontinuous volume change is employed. An enhanced strain approach is used to provide the necessary stabilization for the nearly incompressible case. Use of the enhanced strain approach instead of bubbles or a GLS approach avoids inertial terms involving internal element parameters. In the formulation of the element arrays a partial solution is performed at the element level to eliminate the parameters from the enhanced strain and discontinuous volume terms, thus, the element assembled is expressed in terms of nodal displacements and nodal pressures. At material interfaces the pressure should be discontinuous and this may be accomplished by defining a continuous pressure field for the domain of each material separately. No boundary conditions are required for the pressure field in order to obtain stable solutions.

Example solutions are included for a nearly incompressible problems. These include a thick walled cylinder and bending of a cantilever beam composed of nearly incompressible elastic material and a thick walled cylinder for an elastic-plastic material with a Mises type yield function.

2 Equations of Linear Elasticity

2.1 Governing Equations

The behavior of a linear elastic problem in a state of small strain is described by the linear momentum equations

$$\boldsymbol{\nabla} \cdot \boldsymbol{\sigma} + \mathbf{b}_v = \rho\, \ddot{\mathbf{u}} \tag{1}$$

the angular momentum equations

$$\boldsymbol{\sigma} = \boldsymbol{\sigma}^T \tag{2}$$

the strain displacement equations

$$\boldsymbol{\epsilon} = \frac{1}{2}\left(\boldsymbol{\nabla}\mathbf{u} + (\boldsymbol{\nabla}\mathbf{u})^T\right) = \boldsymbol{\nabla}^{(s)}\mathbf{u} \tag{3}$$

the constitutive equations

$$\boldsymbol{\sigma} = \mathbb{C}\,\boldsymbol{\epsilon} + \boldsymbol{\sigma}_0 \tag{4}$$

and boundary and initial conditions. In the above $\mathbf{u}$ is displacement, $\boldsymbol{\sigma}$ is (Cauchy) stress, $\boldsymbol{\sigma}_0$ is an initial known value of stress, $\boldsymbol{\epsilon}$ is strain, $\boldsymbol{\nabla}$ is the gradient operator, $(\cdot)^T$ denotes the transpose, $\mathbb{C}$ are the material moduli, $\mathbf{b}_v$ is the body force per unit volume, and $(\dot{\cdot})$ denotes time differentiation.

The stress and strain may be split into deviatoric and spherical components as

$$\boldsymbol{\sigma} = \boldsymbol{\sigma}_{dev} + \mathbf{1}\, p \tag{5}$$

and

$$\boldsymbol{\epsilon} = \boldsymbol{\epsilon}_{dev} + \frac{1}{3}\mathbf{1}\,\mathrm{tr}\boldsymbol{\epsilon} \tag{6}$$

where $\mathbf{1}$ is the second rank unit tensor,

$$p = \frac{1}{3}\,\mathrm{tr}\,\boldsymbol{\sigma} = \frac{1}{3}\,(\,\sigma_{11} + \sigma_{22} + \sigma_{33}\,) \tag{7}$$

and

$$\mathrm{tr}\,\boldsymbol{\epsilon} = \epsilon_{11} + \epsilon_{22} + \epsilon_{33} \tag{8}$$

The deviatoric components $\boldsymbol{\sigma}_{dev}$ and $\boldsymbol{\epsilon}_{dev}$ may then be deduced to be

$$\boldsymbol{\sigma}_{dev} = \boldsymbol{\sigma} - \frac{1}{3}\mathbf{1}\,\mathrm{tr}\,\boldsymbol{\sigma} \tag{9}$$

and

$$\boldsymbol{\epsilon}_{dev} = \boldsymbol{\epsilon} - \frac{1}{3}\mathbf{1}\,\mathrm{tr}\,\boldsymbol{\epsilon} \tag{10}$$

Introducing the fourth rank tensor operator

$$\mathbf{I}_{dev} = \mathbf{I} - \frac{1}{3}\,\mathbf{1} \otimes \mathbf{1} \tag{11}$$

where $\mathbf{I}$ is the fourth rank unit tensor. The deviatoric quantities may now be written as

$$\boldsymbol{\sigma}_{dev} = \mathbf{I}_{dev} : \boldsymbol{\sigma} \tag{12}$$

and

$$\boldsymbol{\epsilon}_{dev} = \mathbf{I}_{dev} : \boldsymbol{\epsilon} \tag{13}$$

In the above : denotes a double contraction of the tensors

2.2 Matrix Notation

In the above the quantities are given in tensor form. Thus, the components of stress are related to the stress tensor through

$$\boldsymbol{\sigma} = \sigma_{ij}\,\mathbf{e}_i \otimes \mathbf{e}_j \tag{14}$$

where $\mathbf{e}_i$ are unit orthogonal base vectors. The strain tensor may also be written in a similar form to Eq. 14 in terms of the components ϵ_{ij}. In a Cartesian system a position vector in the body may be written in terms of its components x_i as

$$\mathbf{x} = x_i\,\mathbf{e}_i \tag{15}$$

While the above is convenient for writing the equations it is traditional in finite element developments to use a matrix (Voigt) notation. In the matrix form each second rank tensor is written as a vector and each fourth rank tensor as a matrix.

In matrix notation the stress tensor is expanded as

$$\boldsymbol{\sigma} = \begin{bmatrix}\sigma_{11} & \sigma_{22} & \sigma_{33} & \sigma_{12} & \sigma_{23} & \sigma_{31}\end{bmatrix}^T \tag{16}$$

Similarly, the strain tensor is expanded as

$$\begin{aligned} \boldsymbol{\epsilon} &= \begin{bmatrix} \epsilon_{11} & \epsilon_{22} & \epsilon_{33} & \epsilon_{12}+\epsilon_{21} & \epsilon_{23}+\epsilon_{32} & \epsilon_{31}+\epsilon_{31} \end{bmatrix}^T \\ &= \begin{bmatrix} \epsilon_{11} & \epsilon_{22} & \epsilon_{33} & 2\,\epsilon_{12} & 2\,\epsilon_{23} & 2\,\epsilon_{31} \end{bmatrix}^T \end{aligned} \tag{17}$$

The elastic moduli are written in terms of a matrix as

$$\mathbb{C} \rightarrow \mathbf{D} = \begin{bmatrix} D_{11} & D_{12} & D_{13} & D_{14} & D_{15} & D_{16} \\ D_{21} & D_{22} & D_{23} & D_{24} & D_{25} & D_{26} \\ D_{31} & D_{32} & D_{33} & D_{34} & D_{35} & D_{36} \\ D_{41} & D_{42} & D_{43} & D_{44} & D_{45} & D_{46} \\ D_{51} & D_{52} & D_{53} & D_{54} & D_{55} & D_{56} \\ D_{61} & D_{62} & D_{63} & D_{64} & D_{65} & D_{66} \end{bmatrix} \tag{18}$$

Using the above forms, the unit tensors become

$$\mathbf{1} = \begin{bmatrix} 1 & 1 & 1 & 0 & 0 & 0 \end{bmatrix}^T \tag{19}$$

$$\mathbf{I} = \begin{bmatrix} 1 & 0 & 0 & 0 & 0 & 0 \\ 0 & 1 & 0 & 0 & 0 & 0 \\ 0 & 0 & 1 & 0 & 0 & 0 \\ 0 & 0 & 0 & 1 & 0 & 0 \\ 0 & 0 & 0 & 0 & 1 & 0 \\ 0 & 0 & 0 & 0 & 0 & 1 \end{bmatrix} \tag{20}$$

and

$$\mathbf{I}_{dev} = \mathbf{I} - \frac{1}{3}\mathbf{1}\,\mathbf{1}^T = \frac{1}{3}\begin{bmatrix} 2 & -1 & -1 & 0 & 0 & 0 \\ -1 & 2 & -1 & 0 & 0 & 0 \\ -1 & -1 & 2 & 0 & 0 & 0 \\ 0 & 0 & 0 & 1 & 0 & 0 \\ 0 & 0 & 0 & 0 & 1 & 0 \\ 0 & 0 & 0 & 0 & 0 & 1 \end{bmatrix} \tag{21}$$

Thus, in matrix notation

$$\operatorname{tr}\boldsymbol{\epsilon} = \mathbf{1}^T\boldsymbol{\epsilon} \tag{22}$$

3 Variational Structure

3.1 Hu-Washizu Functional for Volumetric Part

The form of the Hu-Washizu variational theorem for the small deformation problem of elastostatics may be written in the form

$$\Pi(\boldsymbol{\epsilon}, \theta, p) = \int_V \left[\, W(\tilde{\boldsymbol{\epsilon}}) + p\left(\mathbf{1}^T\boldsymbol{\epsilon} - \theta\right) \right] dV + \Pi_{ext} = \text{Stationary} \tag{23}$$

In this form, only the volumetric part is expressed in a Hu-Washizu form. The deviatoric part remains in a minimum potential energy form. In Eq. 23 the mixed strain is expressed as

$$\bar{\epsilon} = \epsilon_{dev} + \frac{1}{3}\mathbf{1}\,\theta \tag{24}$$

Taking the variation of the functional given in Eq. 23 yields

$$\delta\Pi = \int_V \left[\left(\delta\epsilon_{dev} + \frac{1}{3}\mathbf{1}\,\delta\theta \right)^T \bar{\sigma} + \delta p \left(\mathbf{1}^T\epsilon - \theta \right) + \left(\mathbf{1}^T\delta\epsilon - \delta\theta \right) p \right] dV + \delta\Pi_{ext} = 0 \tag{25}$$

where the stress as a function of the mixed strain is defined by

$$\bar{\sigma} = \frac{\partial W}{\partial \bar{\epsilon}} \tag{26}$$

Linearization of the first variation leads to a form which will be used subsequently to compute the tangent matrix and is given by

$$\begin{aligned} d\left(\delta\Pi\right) &= \int_V \left[\left(\delta\epsilon + \frac{1}{3}\mathbf{1}\,\delta\theta \right)^T \bar{\mathbf{D}} \left(d\epsilon_{dev} + \frac{1}{3}\mathbf{1}\,d\theta \right) \right. && (27) \\ &+ \left. \delta p \left(\mathbf{1}^T d\epsilon - d\theta \right) + \left(\mathbf{1}^T\delta\epsilon - \delta\theta \right) dp \right] dV && (28) \\ &+ d\left(\delta\Pi_{ext}\right) = 0 && (29) \end{aligned}$$

where $\bar{\mathbf{D}}$ is deduced from the tangent moduli

$$\bar{\mathbb{C}} = \frac{\partial \bar{\sigma}}{\partial \bar{\epsilon}} \tag{30}$$

using Eq. 18. For a hyperelastic material the tangent moduli are deduced from

$$\bar{\mathbb{C}} = \frac{\partial^2 W}{\partial \bar{\epsilon}\,\partial \bar{\epsilon}} \tag{31}$$

3.2 Finite Element Form

A finite element approximation is constructed for the above functional by considering a discretization using 4-node tetrahedral elements. Accordingly, using an isoparametric concept the position in each tetrahedron is expressed in terms of natural coordinates as

$$\mathbf{x}(\boldsymbol{\xi}) = \sum_{\alpha=1}^{4} N_\alpha(\boldsymbol{\xi})\,\hat{\mathbf{x}}^\alpha \tag{32}$$

where $\mathbf{x}$ is a position in an element at a specified natural coordinate, $\hat{\mathbf{x}}^\alpha$ is the position of the α node of the element, $N(\boldsymbol{\xi})$ are shape functions, and $\boldsymbol{\xi}$ are specified natural, volumetric coordinates ordered as

$$\boldsymbol{\xi} = \begin{bmatrix} \xi_1 & \xi_2 & \xi_3 & \xi_4 \end{bmatrix} \tag{33}$$

which have the following properties,

$$0 \leq \xi_\alpha \leq 1 \tag{34}$$

and

$$\xi_1 + \xi_2 + \xi_3 + \xi_4 = 1 \tag{35}$$

For a 4-node (linear) tetrahedron the shape functions are given by

$$N_\alpha(\boldsymbol{\xi}) = \xi_\alpha \tag{36}$$

Using summation convention the position may be written as

$$\mathbf{x}(\boldsymbol{\xi}) = \xi_\alpha \, \hat{\mathbf{x}}^\alpha = \mathbf{N} \, \hat{\mathbf{x}} \tag{37}$$

where

$$\mathbf{N} = \begin{bmatrix} N_1 & N_2 & N_3 & N_4 \end{bmatrix} \tag{38}$$

Similarly, the displacement, volume change, and pressure in each element may be written as

$$\mathbf{u}(\boldsymbol{\xi}) = \xi_\alpha \, \hat{\mathbf{u}}^\alpha = \mathbf{N} \, \hat{\mathbf{u}} \tag{39}$$

$$p(\boldsymbol{\xi}) = \xi_\alpha \, \hat{p}^\alpha = \mathbf{N} \, \hat{\mathbf{p}} \tag{40}$$

and

$$\theta(\boldsymbol{\xi}) = \xi_\alpha \, \hat{\theta}^\alpha = \mathbf{N} \, \hat{\boldsymbol{\theta}} \tag{41}$$

Based upon the above approximation for displacements the strains based on the symmetric gradient of the displacements are computed from

$$\boldsymbol{\epsilon} = \mathbf{B}_\alpha(\boldsymbol{\xi}) \, \hat{\mathbf{u}}^\alpha \tag{42}$$

where for a three dimensional problem expressed in Cartesian coordinates the strain displacement matrix is given by (e.g., [29] or [10])

$$\mathbf{B}_\alpha(\boldsymbol{\xi}) = \begin{bmatrix} \frac{\partial N_\alpha}{\partial x_1} & 0 & 0 \\ 0 & \frac{\partial N_\alpha}{\partial x_2} & 0 \\ 0 & 0 & \frac{\partial N_\alpha}{\partial x_3} \\ \frac{\partial N_\alpha}{\partial x_2} & \frac{\partial N_\alpha}{\partial x_1} & 0 \\ 0 & \frac{\partial N_\alpha}{\partial x_3} & \frac{\partial N_\alpha}{\partial x_2} \\ \frac{\partial N_\alpha}{\partial x_3} & 0 & \frac{\partial N_\alpha}{\partial x_1} \end{bmatrix} \tag{43}$$

For a 4-node (linear) tetrahedron the derivatives may be deduced from

$$\begin{bmatrix} x_1 \\ x_2 \\ x_3 \\ 1 \end{bmatrix} = \begin{bmatrix} \hat{x}_1^1 & \hat{x}_1^2 & \hat{x}_1^3 & \hat{x}_1^4 \\ \hat{x}_2^1 & \hat{x}_2^2 & \hat{x}_2^3 & \hat{x}_2^4 \\ \hat{x}_3^1 & \hat{x}_3^2 & \hat{x}_3^3 & \hat{x}_3^4 \\ 1 & 1 & 1 & 1 \end{bmatrix} \begin{bmatrix} \xi_1 \\ \xi_2 \\ \xi_3 \\ \xi_4 \end{bmatrix} \tag{44}$$

In the development considered here an enhanced strain formulation will be employed in which the mixed strain will be taken in the form

$$\bar{\boldsymbol{\epsilon}} = \mathbf{I}_{dev}\,(\mathbf{B}_\alpha\,\hat{\mathbf{u}}^\alpha + \boldsymbol{\epsilon}_e) + \frac{1}{3}\mathbf{1}\,\theta \tag{45}$$

where $\boldsymbol{\epsilon}_e$ is an assumed enhanced strain. For the element considered here the enhanced strain terms are deduced from the symmetric gradient of a *bubble mode*. Accordingly, the bubble mode is expressed as

$$N_e(\boldsymbol{\xi}) = \xi_1\,\xi_2\,\xi_3\,\xi_4 \tag{46}$$

and the enhanced strain is given by

$$\boldsymbol{\epsilon}_e(\boldsymbol{\xi}) = \mathbf{B}_e(\boldsymbol{\xi})\,\hat{\mathbf{u}}_e \tag{47}$$

where $\hat{\mathbf{u}}_e$ are three enhanced strain parameters and $\mathbf{B}_e$ is computed using Eqs. 43 and 46.

The enhanced strain may now be deduced from

$$\bar{\boldsymbol{\epsilon}} = \mathbf{I}_{dev}\,(\mathbf{B}_u\,\hat{\mathbf{u}} + \mathbf{B}_e\,\hat{\mathbf{u}}_e) + \frac{1}{3}\mathbf{1}\,\theta \tag{48}$$

where

$$\mathbf{B}_u = \begin{bmatrix}\mathbf{B}_1 & \mathbf{B}_2 & \mathbf{B}_3 & \mathbf{B}_4\end{bmatrix} \tag{49}$$

and

$$\hat{\mathbf{u}} = \begin{bmatrix}\hat{\mathbf{u}}_1 & \hat{\mathbf{u}}_2 & \hat{\mathbf{u}}_3 & \hat{\mathbf{u}}_4\end{bmatrix}^T \tag{50}$$

Using the above, the first term in the variational equation Eq. 25 becomes

$$\begin{bmatrix}\delta\hat{\mathbf{u}} & \delta\hat{\mathbf{u}}_e & \delta\hat{\mathbf{p}} & \delta\hat{\theta}\end{bmatrix}\begin{bmatrix}\mathbf{R}_u\\ \mathbf{R}_e\\ \mathbf{R}_p\\ \mathbf{R}_\theta\end{bmatrix} = \delta\hat{\mathbf{a}}^T\mathbf{R} \tag{51}$$

where

$$\mathbf{R}_u = \int_{V_e}\mathbf{B}_u^T\,[\,\mathbf{I}_{dev}\,\bar{\boldsymbol{\sigma}} + \mathbf{1}\,p\,]\,dV \tag{52}$$

$$\mathbf{R}_e = \int_{V_e}\mathbf{B}_e^T\,[\,\mathbf{I}_{dev}\,\bar{\boldsymbol{\sigma}} + \mathbf{1}\,p\,]\,dV \tag{53}$$

$$\mathbf{R}_p = \int_{V_e}\mathbf{N}^T\left[\mathbf{1}^T\,(\mathbf{B}_u\,\hat{\mathbf{u}} + \mathbf{B}_e\,\hat{\mathbf{u}}_e) - \theta\right]\,dV \tag{54}$$

$$\mathbf{R}_\theta = \int_{V_e}\mathbf{N}^T\left[\frac{1}{3}\mathbf{1}^T\bar{\boldsymbol{\sigma}} - p\right]\,dV \tag{55}$$

In the above p and θ are computed from Eqs. 40 and 41, respectively, and $\bar{\boldsymbol{\sigma}}$ from Eq. 26. Introducing the notation

$$\bar{\theta} = \mathbf{1}^T\,(\mathbf{B}_u\,\hat{\mathbf{u}} + \mathbf{B}_e\hat{\mathbf{u}}_e) \tag{56}$$

$$\bar{p} = \frac{1}{3}\mathbf{1}^T\bar{\boldsymbol{\sigma}} \tag{57}$$

$$\tilde{\boldsymbol{\sigma}} = \bar{\boldsymbol{\sigma}} + (p - \bar{p})\,\mathbf{1} \tag{58}$$

the variational terms become

$$\mathbf{R}_u = \int_{V_e} \mathbf{B}_u^T \tilde{\boldsymbol{\sigma}}\, dV \tag{59}$$

$$\mathbf{R}_e = \int_{V_e} \mathbf{B}_e^T \tilde{\boldsymbol{\sigma}}\, dV \tag{60}$$

$$\mathbf{R}_p = \int_{V_e} \mathbf{N}^T \left[\bar{\theta} - \theta\right]\, dV \tag{61}$$

$$\mathbf{R}_\theta = \int_{V_e} \mathbf{N}^T \left[\bar{p} - p\right]\, dV \tag{62}$$

Linearization of the residual for use in a Newton solution algorithm gives

$$\mathbf{K}\,\Delta\mathbf{a} = \mathbf{f} - \mathbf{R} \tag{63}$$

where

$$\Delta\hat{\mathbf{a}} = \left[\Delta\hat{\mathbf{u}} \quad \Delta\hat{\mathbf{u}}_e \quad \Delta\hat{\mathbf{p}} \quad \Delta\hat{\boldsymbol{\theta}}\right]^T \tag{64}$$

and $\mathbf{f}$ are forces from the $\delta\Pi_{ext}$ term. This ordering yields the tangent tensor

$$\mathbf{K} = \begin{bmatrix} \mathbf{K}_{uu} & \mathbf{K}_{ue} & \mathbf{K}_{up} & \mathbf{K}_{u\theta} \\ \mathbf{K}_{eu} & \mathbf{K}_{ee} & \mathbf{K}_{ep} & \mathbf{K}_{e\theta} \\ \mathbf{K}_{pu} & \mathbf{K}_{pe} & \mathbf{0} & \mathbf{K}_{p\theta} \\ \mathbf{K}_{\theta u} & \mathbf{K}_{\theta e} & \mathbf{K}_{\theta p} & \mathbf{K}_{\theta\theta} \end{bmatrix} \tag{65}$$

where

$$\mathbf{K}_{uu} = \int_{V_e} \mathbf{B}_u^T \bar{\mathbf{D}}_{11}\, \mathbf{B}_u\, dV \tag{66}$$

$$\mathbf{K}_{up} = \int_{V_e} \mathbf{B}_u^T \mathbf{1}\, \mathbf{N}\, dV = \mathbf{K}_{pu}^T \tag{67}$$

$$\mathbf{K}_{u\theta} = \int_{V_e} \mathbf{B}_u^T \bar{\mathbf{D}}_{12}\, \mathbf{N}\, dV = \mathbf{K}_{\theta u}^T \tag{68}$$

$$\mathbf{K}_{p\theta} = -\int_{V_e} \mathbf{N}^T \mathbf{N}\, dV = \mathbf{K}_{\theta p}^T \tag{69}$$

$$\mathbf{K}_{\theta\theta} = \int_{V_e} \mathbf{N}^T \bar{\mathbf{D}}_{22}\, \mathbf{N}\, dV \tag{70}$$

The terms related to the enhanced modes may be obtained by substituting $\mathbf{B}_e$ for $\mathbf{B}_u$ in the appropriate positions.

The mixed form of the material parameters for symmetric moduli are computed as

$$\bar{\mathbf{D}}_{11} = \mathbf{I}_{dev}\, \bar{\mathbf{D}}\, \mathbf{I}_{dev} \tag{71}$$

$$\bar{\mathbf{D}}_{12} = \frac{1}{3}\mathbf{I}_{dev}\, \bar{\mathbf{D}}\, \mathbf{1} = \bar{\mathbf{D}}_{21}^T \tag{72}$$

$$\bar{\mathbf{D}}_{22} = \frac{1}{9}\mathbf{1}^T \bar{\mathbf{D}}\, \mathbf{1} \tag{73}$$

4 Finite Deformation Formulation

A variational form for the finite deformation hyperelastic problem is given by

$$\Pi = \int_V \left[W(\bar{\mathbf{C}}) + p\,(J - \theta) \right] dV + \Pi_{ext} \tag{74}$$

where p is the mixed pressure in the current (deformed) configuration, J is the determinant of the deformation gradient $\mathbf{F}$, θ is the mixed volume in the current configuration, W is the stored energy function expressed in terms of the mixed right Green deformation tensor $\bar{\mathbf{C}}$, and Π_{ext} is the functional for the body loading and boundary terms. This form of the variational problem has been used previously for problems formulated in principal stretches [23]. Here we use the form without referring to the specific structure of the stored energy function. In particular we wish to admit forms in which the volumetric and deviatoric parts are not split as in Reference [23].

The mixed right Green deformation tensor is expressed as

$$\bar{\mathbf{C}} = \bar{\mathbf{F}}^T \bar{\mathbf{F}} \tag{75}$$

where

$$\bar{\mathbf{F}} = \left(\frac{\theta}{J} \right)^{\frac{1}{3}} \mathbf{F} \tag{76}$$

The variation of Eq. 74 is given by

$$\delta\Pi = \int_V \left[\frac{\partial W}{\partial \bar{\mathbf{C}}} : \delta\bar{\mathbf{C}} + \delta p\,(J - \theta) + p\,(\delta J - \delta\theta) \right] dV + \delta\Pi_{ext} \tag{77}$$

A second Piola-Kirchhoff stress is related to the derivative of the stored energy function through

$$\bar{\mathbf{S}} = 2 \frac{\partial W}{\partial \bar{\mathbf{C}}} \tag{78}$$

The first term on the right side of Eq. 77 now may be written as

$$\delta\Pi_{int} = \int_V \frac{1}{2} \left(\bar{\mathbf{S}} : \delta\bar{\mathbf{C}} \right) dV \tag{79}$$

The variation of the mixed deformation gradient $\bar{\mathbf{C}}$ is given by

$$\delta\bar{\mathbf{C}} = \left(\frac{\theta}{J} \right)^{\frac{2}{3}} \delta\mathbf{C} + \frac{2}{3} \left(\frac{\delta\theta}{\theta} - \frac{\delta J}{J} \right) \bar{\mathbf{C}} \tag{80}$$

where

$$\delta J = \frac{1}{2} J\, \mathbf{C}^{-1} : \delta\mathbf{C} \tag{81}$$

which gives

$$\delta\bar{\mathbf{C}} = \frac{2}{3} \frac{\delta\theta}{\theta} \bar{\mathbf{C}} + \left(\frac{\theta}{J} \right)^{\frac{2}{3}} \left[\mathbf{I} - \frac{1}{3}\, \mathbf{C} \otimes \mathbf{C}^{-1} \right] : \delta\mathbf{C} \tag{82}$$

Using the above, Eq. 79 may be expressed in terms of quantities on the current configuration as

$$\delta\Pi_{int} = \int_V \left(\frac{\delta\theta}{\theta}\,\bar{p} + \boldsymbol{\nabla}^{(s)}\delta\mathbf{u} : \bar{\boldsymbol{\sigma}} \right) \theta\, dV \tag{83}$$

where $\boldsymbol{\nabla}^{(s)}$ denotes the symmetric part of the gradient, the Cauchy stress is given by

$$\bar{\boldsymbol{\sigma}} = \frac{1}{\theta}\,\bar{\mathbf{F}}\,\bar{\mathbf{S}}\,\bar{\mathbf{F}}^T \tag{84}$$

the pressure is given by

$$\bar{p} = \frac{1}{3}\,\mathrm{tr}\,\bar{\boldsymbol{\sigma}} \tag{85}$$

and

$$\delta J = J\,\mathrm{div}\,\delta\mathbf{u} \tag{86}$$

in which div is the divergence operator.

4.1 Finite Elements: Matrix Notation

The current configuration may be expressed in terms of a displacement $\mathbf{u}$ from the reference configuration coordinates $\mathbf{X}$ as[1]

$$\mathbf{x} = \mathbf{X} + \mathbf{u} \tag{87}$$

A finite element interpolation for the reference configuration of each element is given by

$$\mathbf{X} = \xi_\alpha\,\hat{\mathbf{X}}^\alpha = \mathbf{N}\,\hat{\mathbf{X}} \tag{88}$$

with the remaining interpolations as for the small deformation case. We again assume that the interpolations for $\mathbf{u}$ and p are C^0 continuous while those for θ are discontinuous between elements. With this form the parameters $\hat{\mathbf{u}}$ and $\hat{\mathbf{p}}$ are nodal variables and $\hat{\mathbf{u}}_e$ and $\hat{\boldsymbol{\theta}}$ are associated with an individual element. The deformation gradient for the finite element approximation is taken as

$$\mathbf{F} = \mathbf{1} + \frac{\partial\mathbf{u}}{\partial\mathbf{X}} + \mathbf{F}_e \tag{89}$$

where $\mathbf{F}_e$ is an enhanced deformation gradient. In the developments considered here the enhanced deformation gradient is computed from

$$\mathbf{F}_e = \frac{\partial\mathbf{u}_e}{\partial\mathbf{X}} = \frac{\partial N_e}{\partial\mathbf{X}}\hat{\mathbf{u}}_e \tag{90}$$

in which the shape function on a tetrahedron for the enhanced mode is again the *bubble function*

$$N_e = \xi_1\,\xi_2\,\xi_3\,\xi_4 \tag{91}$$

[1] An abuse in notation which does not distinguish between the reference and current configuration is used (i.e., no shifter is included).

and $\mathbf{u}_e$ are element parameters[2]. The deformation gradient may now be written as

$$\mathbf{F} = \mathbf{1} + \frac{\partial \mathbf{N}}{\partial \mathbf{X}} \hat{\mathbf{u}} + \frac{\partial N_e}{\partial \mathbf{X}} \hat{\mathbf{u}}_e \tag{92}$$

where

$$\mathbf{u} = \begin{bmatrix} \hat{\mathbf{u}}_1 & \hat{\mathbf{u}}_2 & \hat{\mathbf{u}}_3 & \hat{\mathbf{u}}_4 \end{bmatrix}^T \tag{93}$$

4.2 Residual: Matrix Notation

Using the above notation, Eq. 83 may be expressed in matrix form as

$$\begin{aligned} \delta\Pi &= \delta\hat{\mathbf{u}}^T \int_V \mathbf{B}_u^T \tilde{\boldsymbol{\sigma}}\, \theta \, dV \\ &+ \delta\hat{\mathbf{u}}_e^T \int_V \mathbf{B}_e^T \tilde{\boldsymbol{\sigma}}\, \theta \, dV \\ &+ \delta\hat{\mathbf{p}}^T \int_V \mathbf{N}^T \, (J - \theta) \, dV \\ &+ \delta\hat{\theta}^T \int_V \mathbf{N}^T \, (\bar{p} - p) \, dV + \delta\Pi_{ext} \end{aligned} \tag{94}$$

In this form of the finite deformation problem $\mathbf{B}_u$ and $\mathbf{B}_e$ have the same form as in the small deformation strain displacement matrix. Also,

$$\tilde{\boldsymbol{\sigma}} = \bar{\boldsymbol{\sigma}} + (\tilde{p} - \bar{p}) \, \mathbf{1} \tag{95}$$

where

$$\tilde{p} = \frac{J}{\theta} p \tag{96}$$

Thus, the finite element arrays for the first variation terms are given by

$$\mathbf{R}_u = \int_V \mathbf{B}_u^T \tilde{\boldsymbol{\sigma}}\, \theta \, dV \tag{97}$$

$$\mathbf{R}_e = \int_V \mathbf{B}_e^T \tilde{\boldsymbol{\sigma}}\, \theta \, dV \tag{98}$$

$$\mathbf{R}_p = \int_V \mathbf{N}^T \, (J - \theta) \, dV \tag{99}$$

$$\mathbf{R}_\theta = \int_V \mathbf{N}^T \, (\bar{p} - p) \, dV \tag{100}$$

Inertial terms may be added to the above using the d'Alembert principle. Since the finite element displacement field does not involve the enhanced term, there are no inertial terms involving the parameter $\mathbf{u}_e$. With the inertial terms added the residual expression for $\mathbf{R}_u$ is given by

$$\mathbf{R}_u = \int_V \left(\mathbf{B}_u^T \tilde{\boldsymbol{\sigma}}\, \theta + \rho_0 \mathbf{N}^T \mathbf{N}\, \ddot{\mathbf{u}} \right) dV \tag{101}$$

[2]The element parameters have dimensions of displacement; however, as enhanced functions they do not influence the displacement approximation.

where ρ_0 is the reference configuration mass density. This greatly simplifies the solution process for transient problems. However, since there are no inertial effects for the enhanced, pressure and volume terms it is necessary to always use an implicit scheme for these terms. An explicit method may be employed to solve the momentum equation (i.e., the equation associated with the parameters $\hat{\mathbf{u}}$ in Eq. 94. Here we only consider a fully implicit scheme which is applicable to either transient or static problems.

4.3 Tangent Stiffness: Matrix Notation

A Newton scheme as defined by Eqs. 63 to 65 may be employed to solve Eq. 94. To construct the tangent matrix $\mathbf{K}$ it is necessary to linearize Eq. 77. The linearization may be assembled as

$$\begin{aligned}\Delta\left(\delta\Pi\right) &= \int_V \left[\delta\bar{\mathbf{C}} : \frac{\partial^2 W}{\partial\bar{\mathbf{C}}\,\partial\bar{\mathbf{C}}} : \Delta\bar{\mathbf{C}} + \Delta\left(\delta\bar{\mathbf{C}}\right) : \frac{\partial W}{\partial\bar{\mathbf{C}}}\right] dV + \int_V p\,\Delta\left(\delta J\right)\,dV \\ &+ \int_V \delta p\,\left(\Delta J - \Delta\theta\right)\,dV + \int_V \Delta p\,\left(\delta J - \delta\theta\right)\,dV + \Delta\left(\delta\Pi_{ext}\right) \qquad (102)\end{aligned}$$

where $\Delta\bar{\mathbf{C}}$, Δp, etc., denote incremental quantities and the material tangent moduli are denoted by

$$\bar{\mathbb{C}} = 4\frac{\partial^2 W}{\partial\bar{\mathbf{C}}\,\partial\bar{\mathbf{C}}} \qquad (103)$$

Using this and the linearization of $\bar{\mathbf{C}}$ the first two integrals in Eq. 102 may be written in matrix form as

$$\Delta\left(\delta\Pi_{int}\right) = \begin{bmatrix}\delta\hat{\mathbf{u}}^T & \delta\hat{\mathbf{u}}_e^T & \delta\hat{\theta}^T\end{bmatrix}\begin{bmatrix}\mathbf{K}_{uu} & \mathbf{K}_{ue} & \mathbf{K}_{u\theta} \\ \mathbf{K}_{eu} & \mathbf{K}_{ee} & \mathbf{K}_{e\theta} \\ \mathbf{K}_{\theta u} & \mathbf{K}_{\theta e} & \mathbf{K}_{\theta\theta}\end{bmatrix}\begin{bmatrix}\Delta\hat{\mathbf{u}} \\ \Delta\hat{\mathbf{u}}_e \\ \Delta\hat{\theta}\end{bmatrix} \qquad (104)$$

These tangent terms may be split into two parts as

$$\mathbf{K}_{ij} = \mathbf{K}_{ij}^{(c)} + \mathbf{K}_{ij}^{(g)} \qquad (105)$$

which correspond to a constitutive part and a geometric part. In the subsequent developments we again note that the structure of the displacement and the enhanced tangent terms are identical (except for the inertial term). It is only necessary to replace $\mathbf{B}_u$ by $\mathbf{B}_e$ and $\mathbf{N}$ by N_e in the appropriate locations.

The spatial tangent of a constitutive model is denoted by

$$\bar{\mathbf{c}} = \frac{1}{\theta}\bar{\mathbf{F}}\bar{\mathbf{F}}\,\bar{\mathbb{C}}\bar{\mathbf{F}}^T\bar{\mathbf{F}}^T \qquad (106)$$

and the constitutive tangent terms for symmetric moduli are expressed as

$$\mathbf{K}_{uu}^{(c)} = \int_V \mathbf{B}_u^T\bar{\mathbf{D}}_{11}\mathbf{B}_u\,\theta\,dV \qquad (107)$$

$$\mathbf{K}_{u\theta}^{(c)} = \int_V \mathbf{B}_u^T\bar{\mathbf{D}}_{12}\mathbf{N}_\theta\,\theta\,dV = \mathbf{K}_{\theta u}^{(c)T} \qquad (108)$$

$$\mathbf{K}_{\theta\theta}^{(c)} = \int_V \mathbf{N}_\theta^T\bar{\mathbf{D}}_{22}\mathbf{N}_\theta\,\theta\,dV \qquad (109)$$

where

$$\mathbf{N}_\theta = \frac{1}{\theta}\mathbf{N} \tag{110}$$

and in matrix notation

$$\begin{aligned}
\bar{\mathbf{D}}_{11} &= \mathbf{I}_{dev}\bar{\mathbf{D}}\,\mathbf{I}_{dev} \\
&- \frac{2}{3}\left(\mathbf{1}\bar{\boldsymbol{\sigma}}_{dev}^T + \bar{\boldsymbol{\sigma}}_{dev}\mathbf{1}^T\right) + 2\,(\bar{p}-\tilde{p})\,\mathbb{I} - \left(\frac{2}{3}\bar{p}-\tilde{p}\right)\mathbf{1}\mathbf{1}^T
\end{aligned} \tag{111}$$

$$\bar{\mathbf{D}}_{12} = \frac{1}{3}\mathbf{I}_{dev}\bar{\mathbf{D}}\,\mathbf{1} + \frac{2}{3}\bar{\boldsymbol{\sigma}}_{dev} = \bar{\mathbf{D}}_{21}^T \tag{112}$$

$$\bar{\mathbf{D}}_{22} = \frac{1}{9}\mathbf{1}^T\bar{\mathbf{D}}\,\mathbf{1} - \frac{1}{3}\bar{p} \tag{113}$$

In the above, $\bar{\mathbf{c}}$ has been transformed to $\bar{\mathbf{D}}$ using Eq. 18 and $\mathbb{I}$ is the matrix form of the fourth rank identity tensor,

$$2\,\mathbb{I} = \begin{bmatrix} 2 & 0 & 0 & 0 & 0 & 0 \\ 0 & 2 & 0 & 0 & 0 & 0 \\ 0 & 0 & 2 & 0 & 0 & 0 \\ 0 & 0 & 0 & 1 & 0 & 0 \\ 0 & 0 & 0 & 0 & 1 & 0 \\ 0 & 0 & 0 & 0 & 0 & 1 \end{bmatrix} \tag{114}$$

The geometric tangent term is given by

$$\mathbf{K}_{uu}^{(g)} = \int_V (\boldsymbol{\nabla}\mathbf{N} : \tilde{\boldsymbol{\sigma}}\,\boldsymbol{\nabla}\mathbf{N})\,\mathbf{I}\,\theta\,dV \tag{115}$$

where $\mathbf{I}$ is a 3×3 identity matrix and $\boldsymbol{\nabla}\mathbf{N}$ as the spatial gradient of the shape functions with components $\frac{\partial N_a}{\partial x_j}$. Again, the geometric tangent for the enhanced effects is obtained by substituting $\boldsymbol{\nabla}\mathbf{N}$ by $\boldsymbol{\nabla}N_e$.

The last two integrals in Eq. 102 are given by

$$\Delta\left(\delta\Pi_{mix}\right) = \int_V \delta p\,\left(\Delta J - \Delta\theta\right)\,dV + \int_V \left(\delta J - \delta\theta\right)\,\Delta p\,dV \tag{116}$$

In matrix form these may be written as

$$d\left(\delta\Pi_{mix}\right) = \begin{bmatrix} \delta\hat{\mathbf{u}}^T & \delta\hat{\mathbf{u}}_e^T & \delta\hat{\mathbf{p}} & \delta\hat{\theta}^T \end{bmatrix} \begin{bmatrix} \mathbf{0} & \mathbf{0} & \mathbf{K}_{up}^{(m)} & \mathbf{0} \\ \mathbf{0} & \mathbf{0} & \mathbf{K}_{ep}^{(m)} & \mathbf{0} \\ \mathbf{K}_{pu}^{(m)} & \mathbf{K}_{pe}^{(m)} & \mathbf{0} & \mathbf{K}_{p\theta}^{(m)} \\ \mathbf{0} & \mathbf{0} & \mathbf{K}_{\theta p}^{(m)} & \mathbf{0} \end{bmatrix} \begin{bmatrix} \Delta\hat{\mathbf{u}} \\ \Delta\hat{\mathbf{u}}_e \\ \Delta\hat{\mathbf{p}} \\ \Delta\hat{\theta} \end{bmatrix} \tag{117}$$

where

$$\mathbf{K}_{up}^{(m)} = \int_V \mathbf{B}_u^T\mathbf{1}\,\mathbf{N}\,J\,dV = \mathbf{K}_{pu}^{(m)T}dV \tag{118}$$

$$\mathbf{K}_{p\theta}^{(m)} = -\int_V \mathbf{N}^T\mathbf{N}\,dV = \mathbf{K}_{\theta p}^{(m)} \tag{119}$$

5 Solution of Linear Equations

If the interpolation for $\mathbf{u}$ is C^0 continuous in the whole domain, the interpolation for p is C^0 continuous in *each* material, and the interpolation for θ is piece wise continuous, the solution can be performed in two steps. In the first step the parameters for θ and $\mathbf{u}_e$ are eliminated at the element level (by static condensation). If the material is non-linear this requires that the Newton iteration for these parameters be performed before computing the final element arrays. After the iteration, the residuals $\mathbf{f}_\theta - \mathbf{R}_\theta$ and $\mathbf{f}_e - \mathbf{R}_e$ will be zero and the solution may be partitioned in an element as:

$$\begin{bmatrix} \mathbf{K}_{11} & \mathbf{K}_{12} \\ \mathbf{K}_{21} & \mathbf{K}_{22} \end{bmatrix} \begin{bmatrix} \Delta\hat{\mathbf{a}}_1 \\ \Delta\hat{\mathbf{a}}_2 \end{bmatrix} = \begin{bmatrix} \mathbf{R}_1 \\ \mathbf{0} \end{bmatrix} \tag{120}$$

where

$$\mathbf{K}_{11} = \begin{bmatrix} \mathbf{K}_{uu} & \mathbf{K}_{up} \\ \mathbf{K}_{pu} & \mathbf{0} \end{bmatrix} \tag{121}$$

$$\mathbf{K}_{12} = \begin{bmatrix} \mathbf{K}_{u\theta} & \mathbf{K}_{ue} \\ \mathbf{K}_{p\theta} & \mathbf{K}_{pe} \end{bmatrix} = \mathbf{K}_{21}^T \tag{122}$$

$$\mathbf{K}_{22} = \begin{bmatrix} \mathbf{K}_{\theta\theta} & \mathbf{K}_{\theta e} \\ \mathbf{K}_{e\theta} & \mathbf{K}_{ee} \end{bmatrix} \tag{123}$$

$$\mathbf{R}_1 = \begin{bmatrix} \mathbf{f}_u - \mathbf{R}_u \\ \mathbf{f}_p - \mathbf{R}_p \end{bmatrix} \tag{124}$$

$$\Delta\hat{\mathbf{a}}_1 = \begin{bmatrix} \Delta\hat{\mathbf{u}} \\ \Delta\hat{\mathbf{p}} \end{bmatrix} \tag{125}$$

and

$$\Delta\hat{\mathbf{a}}_2 = \begin{bmatrix} \Delta\hat{\boldsymbol{\theta}} \\ \Delta\hat{\mathbf{u}}_e \end{bmatrix} \tag{126}$$

Eliminating the θ and bubble parameters yields the solutions

$$d\hat{\mathbf{a}}_2 = -\mathbf{K}_{22}^{-1}\mathbf{K}_{21} \tag{127}$$

and

$$\mathbf{K}_{11}^{\star}\, d\hat{\mathbf{a}}_1 = \mathbf{R}_1 \tag{128}$$

The reduced tangent is given by

$$\mathbf{K}_{11}^{\star} = \mathbf{K}_{11} - \mathbf{K}_{12}\mathbf{K}_{22}^{-1}\mathbf{K}_{21} \tag{129}$$

Thus, the second part of the solution proceeds by assembling the reduced element matrix and residual into the global equations. This leads to a system of equations to be solved for the incremental parameters associated with the nodal displacement and pressure variables.

6 Example Solutions

Each of the example problems uses a regular block of six tetrahedral elements to form a dodecahedron. This topology permits a direct comparison with hexahedral elements. A typical dodecahedron is shown in Figure 1 with the individual tetrahedra shown separated in Figure 2.

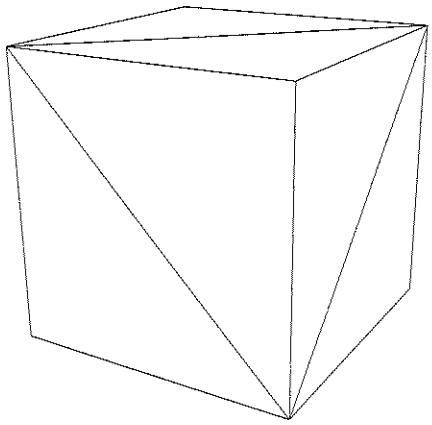

Figure 1: Dodecahedron formed from 6-tetrahedra.

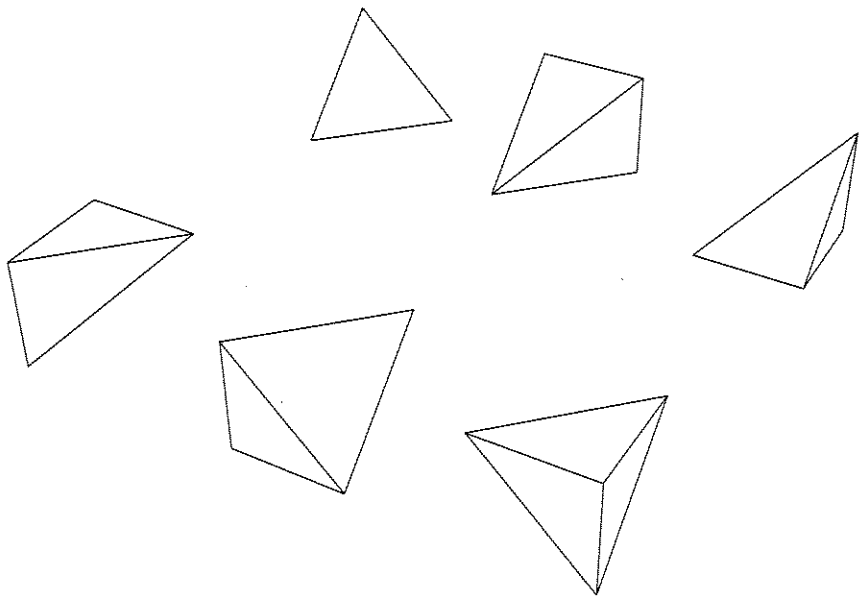

Figure 2: Tetrahedra used to form a dodecahedron.

6.1 Patch Tests

The mesh shown in Figure 1 is used to perform standard constant deformation patch tests. Each is passed since the element is constructed to contain the constant states. However, the patch tests are also used to verify the correctness of the coding for the element arrays.

6.2 Thick Walled Cylinder

An infinitely long thick walled cylinder with inner boundary radius of 5 units and outer boundary radius of 10 units is subjected to an internal pressure of 103.13 (which is $324/\pi$) units. A wedge with unit thickness and a 10-degree angle sector is considered for the finite element analysis using the mixed tetrahedral element as shown in Figure 3. The material properties are taken as isotropic linear elastic with $E = 1000$ and $\nu = 0.4999$ to represent nearly incompressible behavior. This problem has been proposed to by MacNeal and Harter [14] as a test on an elements ability to represent proper behavior for a nearly incompressible material. The mesh of tetrahedra is regular and has $N \times 2 \times 1$ divisions in the radial, tangential and axial directions, respectively. The results for the displacements at the inner and outer radii are reported in Table 1 for $N = 10$, in Table 2 for $N = 20$ and in Table 3 for $N = 30$. The results are also compared to those from a mixed hexahedral element with tri-linear displacement and constant pressure and volume change approximations. It is evident that the tetrahedral element behaves correctly for this test.

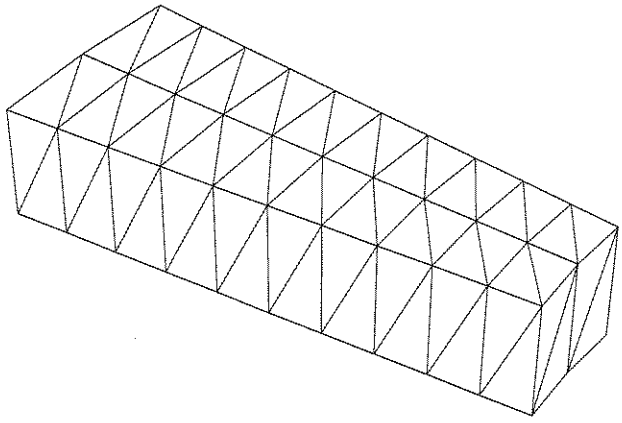

Figure 3: Thick Walled Cylinder Mesh

6.3 Cantilever Beam: Linear Elastic Solution

A cantilever beam with a square cross section and loaded by a line load along the top edge is considered to illustrate the bending capability of the small deformation mixed-enhanced tetrahedral element. The beam has cross-section side lengths of 5 units and length of 50 units. The material properties are taken as $E = 1000$ and $\nu = 0.4999$. These properties represent a nearly incompressible linear elastic behavior. The mesh is uniform with N elements on each

Node	Inner Radius	Outer Radius
1	1.0301	0.5111
2	1.0273	0.5141
3	1.0260	0.5160
4	1.0341	0.5140
5	1.0281	0.5139
6	1.0205	0.5147
Avg	1.0277	0.5140
Hex	1.0312	0.5157
Exact	1.0313	0.5156

Table 1: Thick wall cylinder radial displacement. $N = 10$

Node	Inner Radius	Outer Radius
1	1.0306	0.5127
2	1.0290	0.5152
3	1.0296	0.5163
4	1.0336	0.5154
5	1.0306	0.5148
6	1.0246	0.5153
Avg	1.0297	0.5153
Hex	1.0318	0.5160
Exact	1.0313	0.5156

Table 2: Thick wall cylinder radial displacement. $N = 20$

Node	Inner Radius	Outer Radius
1	1.0306	0.5131
2	1.0294	0.5154
3	1.0304	0.5163
4	1.0331	0.5157
5	1.0312	0.5149
6	1.0256	0.5154
Avg	1.0301	0.5151
Hex	1.0319	0.5160
Exact	1.0313	0.5156

Table 3: Thick wall cylinder radial displacement. $N = 30$

side and $5\,N$ elements along the length. Half of the beam is modeled with a non-uniform distribution along the length, thus, there are only $N/2$ elements in the symmetry direction. All nodes at the fixed end are restrained for each displacement component. No restraints are imposed on the pressure parameters. The mesh for tetrahedral and hexahedral elements for $N = 4$ is shown in Figure 4. The results for the tip displacement are given in Table 4 and compared to a mixed hexahedral element with tri-linear displacements and discontinuous constant pressure and volume change. The results for the mixed element are also shown in Figure 6.3. It is evident that the mixed-enhanced tetrahedral element converges adequately for a low order linear interpolation but has poorer bending capability than the hexahedral element. The locking tendency of the displacement form for the tetrahedral element is also clearly evident from the results tabulated.

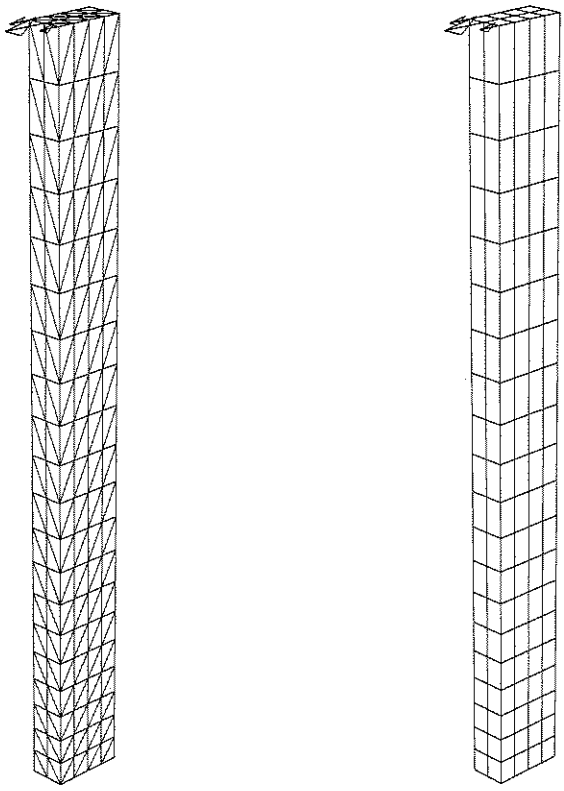

Figure 4: Cantilever Beam: Tetrahedral and Quadrilateral Meshes

6.4 Cantilever Beam: Linear Elasto-Plastic Solution

The cantilever beam considered above is next analyzed assuming an elasto-plastic material behavior. For this analysis the mesh with N equal to 8 is used for analyses with mixed-enhance tetrahedral elements and mixed hexahedral elements. The material parameters are

N	Displ. Tetrahedra	Mixed Tetrahedra	Mixed Hexahedra
2	0.191	5.587	10.447
4	0.233	9.619	11.947
6	0.298	11.042	12.310
8	0.384	11.674	12.448
10	0.489	11.993	12.516

Table 4: Cantilever beam displacement

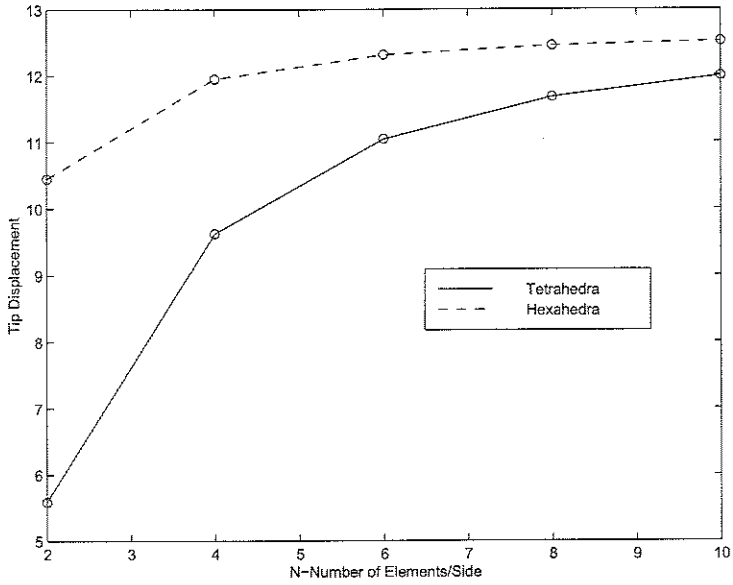

Figure 5: Cantilever Beam: Tip Displacement

taken as $E = 1000$, $\nu = 0.3$, a Mises yield function with perfectly plastic behavior and a uniaxial yield stress $\sigma_Y = 50$.

The left top edge of the cantilever beam is loaded by a uniform displacement with increments of 5-units for each step. Sixteen steps of loading are used and results for the total reaction versus the displacement are shown in Figure 6.

6.5 Cantilever Beam: Finite Elastic Solution

The final example is again the cantilever beam; however, the behavior is now assumed to have finite deformations. For this problem the beam is again loaded by a uniform edge displacement along the left top of the cantilever. A hyperelastic compressible neo-Hookean material with parameters K and G for the volumetric and deviatoric behavior is used. These parameters coincide with the bulk and shear modulus of a small deformation model and are computed from $E = 1000$ and $\nu = 0.4999$. Displacement increments of 5 units are applied

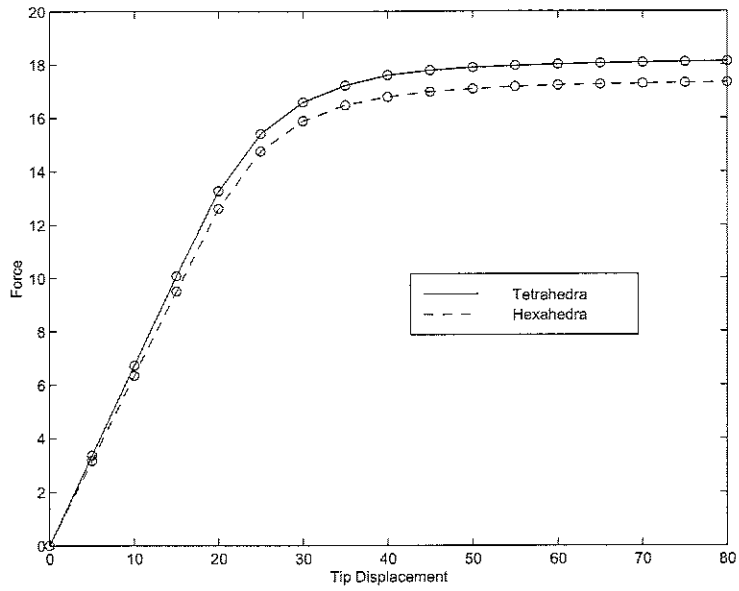

Figure 6: Cantilever Beam: Tip Reaction for Elasto-Plastic Solution

and deformed positions after four and eight steps are shown in Figure 7.

7 Closure

A mixed-enhanced method using tetrahedral elements to solve problems in solid mechanics has been presented. The formulation is applicable to both small and large deformation applications involving elastic and/or inelastic material behavior. The examples presented above illustrate the performance of the element in situations where nearly incompressible behavior is encountered. While acceptable results can be obtained it is evident that the element will only be effective in situations where automatic meshing using tetrahedral elements is available. Finally, the reader is reminded that for multimaterial analyses it will be necessary to permit the pressure interpolations to be discontinuous at material interfaces.

References

[1] J.H. Argyris. Matrix analysis of three-dimensional elastic media – small and large displacements. *Journal of AIAA*, 3:45–51, January 1965.

[2] J.H. Argyris. Three-dimensional anisotropic and inhomogeneous media – matrix analysis for small and large displacements. *Ingenieur Archiv*, 34:33–55, 1965.

[3] D.N. Arnold, F. Brezzi, and M. Fortin. A stable finite element for the stokes equations. *Calcolo*, 21:337–344, 1984.

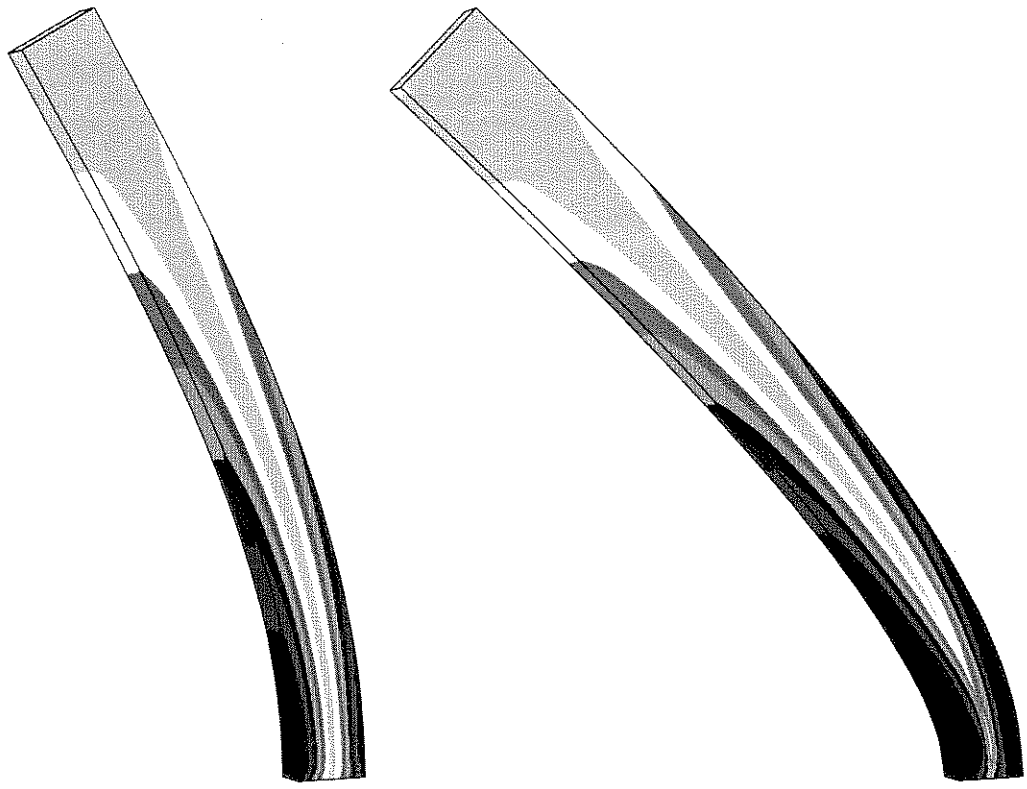

Figure 7: Cantilever Beam: Deformed Mesh at Steps 4 and 8

[4] K.J. Arrow, L. Hurwicz, and H. Uzawa. *Studies in Non-Linear Programming.* Stanford University Press, Stanford, CA, 1958.

[5] J. Bonet and A.J. Burton. A simple average nodal pressure tetrahedral element for incompressible and nearly incompressible dynamic explicit applications. *Communications in Numerical Methods in Engineering*, 14:437–449, 1998.

[6] F. Brezzi. On the existence, uniqueness and approximation of saddle-point problems arising from lagrange multipliers. *Rev. Française d'Automatique Inform. Rech. Opér., Ser. Rouge Anal. Numér.*, 8(R-2):129–151, 1974.

[7] A.J. Chorin. A numerical method for solving incompressible viscous problems. *Journal of Computational Physics*, 2:12–26, 1967.

[8] R. Courant. Variational methods for the solution of problems of equilibrium and vibration. *Bulletin of the American Math Society*, 49:1–61, 1943.

[9] R.H. Gallagher, J. Padlog, and P.P. Bijlaard. Stress analysis of heated complex shapes. *ARS Journal*, 29:700–707, 1962.

[10] T.J.R. Hughes. *The Finite Element Method: Linear Static and Dynamic Analysis.* Prentice-Hall, Englewood Cliffs NJ, 1987.

[11] T.J.R. Hughes and L.P. Franca. A new finite element formulation for computational fluid dynamics: Vii. the stokes problem with various well-posed obundary conditions: Symmetric formulation that converge for all velocity/pressure spaces. *Computer Methods in Applied Mechanics and Engineering*, 65:85–96, 1987.

[12] T.J.R. Hughes, L.P. Franca, and M. Balestra. A new finite element formulation for computational fluid dynamics: V. circumventing the babuška-brezzi condition: A stable petrov-galerkin formulation of the stokes problem accomodating equal-order interpolations. *Computer Methods in Applied Mechanics and Engineering*, 59:85–99, 1986.

[13] Babuška I. Error bounds for finite element methods. *Numer. Math.*, 16:322–333, 1971.

[14] R.H. MacNeal and R.L. Harter. A proposed standard set of problems to test finite element accuracy. *Journal of Finite Elements in Analysis and Design*, 1:3–20, 1985.

[15] R.J. Melosh. Structural analysis of solids. *ASCE Structural Journal*, 4:205–223, August 1963.

[16] Y.R. Rashid and W. Rockenhauser. Pressure vessel analysis by finite element techniques. In *Proceedings of Conference on Prestressed Concrete Pressure Vessels*, Institute of Civil Engineering, 1968.

[17] E. Reissner. On a variational theorem in elasticity. *Journal of Mathematics and Physics*, 29(2):90–95, 1950.

[18] J.G. Rice and R.J. Schnipke. An equal-order velocity-pressure formulation that does not exhibit spurious pressure modes. *Computer Methods in Applied Mechanics and Engineering*, 58:135–149, 1986.

[19] G.E. Schneider, G.D. Raithby, and M.M. Yovanovich. Finite element analysis of incompressible flow incorporating equal order pressure and velocity interpolation. In C. Taylor et. al., editor, *Numerical Methods in Laminar and Turbulent Flow*, Plymouth, 1978. Pentech Press.

[20] J.C. Simo and F. Armero. Geometrically non-linear enhanced strain mixed methods and the method of incompatible modes. *International Journal for Numerical Methods in Engineering*, 33:1413–1449, 1992.

[21] J.C. Simo, F. Armero, and R.L. Taylor. Improved versions of assumed enhanced strain tri-linear elements for 3d finite deformation problems. *Computer Methods in Applied Mechanics and Engineering*, 110:359–386, 1993.

[22] J.C. Simo and M.S. Rifai. A class of mixed assumed strain methods and the method of incompatible modes. *International Journal for Numerical Methods in Engineering*, 29:1595–1638, 1990.

[23] J.C. Simo and R.L. Taylor. Quasi-incompressible finite elasticity in principal stretches. continuum basis and numerical algorithms. *Computer Methods in Applied Mechanics and Engineering*, 85:273–310, 1991.

[24] M.J. Turner, R.W. Clouth, H.C. Martin, and L.J. Topp. Stiffness and deflection analysis of complex structures. *Journal of the Aeronautical Sciences*, 23:805–823, 1956.

[25] K. Washizu. *Variational Methods in Elasticity and Plasticity.* Pergamon Press, New York, 3 edition, 1982.

[26] O.C. Zienkiewicz and R. Codina. A general algorithm for compressible and incompressible flow – part i: The split, characteristic-based scheme. *International Journal for Numerical Methods in Fluids*, 20:869–885, 1995.

[27] O.C. Zienkiewicz, K. Morgan, B.V.K. Satya Sai, R. Codina, and M. Vasquez. A general algorithm for compressible and incompressible flow – part ii: Tests on the explicit form. *International Journal for Numerical Methods in Fluids*, 20:887–913, 1995.

[28] O.C. Zienkiewicz, J. Rojek, R.L. Taylor, and M. Pastor. Triangles and tetrahedra in explicit dynamics codes for solids. *International Journal for Numerical Methods in Engineering*, 43:565–583, 1998.

[29] O.C. Zienkiewicz and R.L. Taylor. *The Finite Element Method*, volume 1. McGraw-Hill, London, 4th edition, 1989.